# Osmium Hydrazido and Dinitrogen Complexes

**George M. Coia, Martin Devenney, Peter S. White, and Thomas J. Meyer***

Department of Chemistry, Venable and Kenan Laboratories, The University of North Carolina, Chapel Hill, North Carolina 27599-3290

**David A. Wink**

Chemistry Section, Laboratory of Comparative Carcinogenesis, National Cancer Institute, Frederick Cancer Research and Development Center, Frederick, Maryland 21702

*Received August 22, 1996*[⊗]

$[Os(tpy)(bpy)(NH_3)](PF_6)_2$ **(1)** was oxidized electrochemically in the presence of a series of amines in aqueous solutions buffered to pH 7. With secondary aliphatic amines, electrolysis gave $[Os(tpy)(bpy)(NNR_2)](PF_6)_3$ **(3)**; number of electrons $n = 4.6-5.0$. **3** was reduced to $[Os(tpy)(bpy)(NNR_2)](PF_6)_2$ **(2)** in aqueous and nonaqueous solutions with $n = 1.0$. The structures of **2** were determined by X-ray crystallography for $NR_2$ = diethylamide **(2a)** and morpholide **(2c)** and were found to exhibit bent hydrazido(2−) coordination (Os−N−N = 137°). The salts crystallized in the triclinic system, space group $P\bar{1}$. For **2a**, $a = 9.004(1)$ Å, $b = 9.796(1)$ Å, $c = 20.710(2)$ Å, $\alpha = 88.78(2)°$, $\beta = 85.43(2)°$, $\gamma = 86.22(2)°$, and $Z = 2$. For **2c**, $a = 9.632(8)$ Å, $b = 21.229(9)$ Å, $c = 9.039(5)$ Å, $\alpha = 97.41(4)°$, $\beta = 94.28(5)°$, $\gamma = 85.07(5)°$, and $Z = 2$. Solutions of **2** were protonated in strongly acidic media to give hydrazido(1−) complexes. The p$K_a$ of the protonated form of **2a** is $0.90 \pm 0.01$. Reduction of **2** in aqueous solutions of pH <1 gave **1** and $NH_2R_2^+$ with $n = 4.0$. At higher pH, there is evidence for an Os(II) hydrazine intermediate. Oxidation of **3** by one electron afforded transiently stable species which decomposed to give $[Os(tpy)(bpy)(NCCH_3)]^{3+}$ in acetonitrile solution. Pseudo-first-order rate constants of $8.1 \pm 0.9$ s$^{-1}$ and $0.200 \pm .005$ s$^{-1}$ were estimated by cyclic voltammetry on solutions of **2a** and **2b** ($NR_2$ = piperidide), respectively. Oxidation of **1** at pH 7, in the presence of primary aliphatic amines or ammonia, occurred with $n = 5.9-6.2$, and generated $[Os^{II}(tpy)(bpy)(N_2)](PF_6)_2$ **(4)**.

## Introduction

Chemically reversible interconversion of ammine and nitro groups in the coordination spheres of ruthenium and osmium has been observed (eq 1). The multielectron character of this reaction has prompted a continuing effort toward understanding its mechanistic details and elucidating key intermediates.[1] Among the proposed intermediates are $M^{IV}$ imido (or nitrene)

$$[M^{II}(tpy)(bpy)(NH_3)]^{2+} + 2H_2O \underset{+6e^-,\,7H^+}{\overset{-6e^-,\,7H^+}{\rightleftharpoons}} [M^{II}(tpy)(bpy)(NO_2)]^{+} \quad (1)$$

M = Ru, Os; tpy = 2,2′:6′,2″-terpyridine, bpy = 2,2′-bipyridine

complexes, $[M(tpy)(bpy)(NH)]^{2+}$. These species are isoelectronic with $[M(tpy)(bpy)(O)]^{2+}$ and are expected to share some of the redox features of their oxo analogs. Due to their reactive nature, the most useful insights have been gained by means of *in situ* generation and trapping. A convenient method is to generate $Os^{IV}$ by oxidation of $[Os(tpy)(bpy)(NH_3)]^{2+}$ **(1)** in aqueous solution.

In a preliminary communication,[2] we reported that electrochemical oxidation of **1** in the presence of a large excess of secondary aliphatic amines led to the formation of $[Os(tpy)(bpy)(NNR_2)](PF_6)_3$ **(3)**, and that **3** was reduced to $[Os(tpy)(bpy)(NNR_2)](PF_6)_2$ **(2)** in aqueous and nonaqueous solutions. The structure of **2a** ($R_2 = Et_2$) was determined by X-ray crystallography and was found to exhibit bent hydrazido(2−) coordination. It was determined that reduction of **2** in aqueous solutions of pH ≈ 1 gave **1** and the free amine. Additionally, evidence was presented for the intervention of an $Os^{II}$ hydrazine intermediate.

We now report general syntheses for a series of terminal hydrazides of osmium, along with their structural, spectral, and electrochemical properties. Also presented are the results of the electrochemical oxidation of **1** in the presence of primary aliphatic amines and ammonia, and the properties of the resulting $Os^{II}$ dinitrogen complex.

## Experimental Section

**Measurements.** Proton NMR spectra were acquired by using Bruker AC200 (200 MHz) and WM250 (250 MHz) spectrometers. For variable temperature studies, a calibration curve of sample temperature *vs* probe temperature was established by measuring the difference in chemical shift ($\Delta\delta$) between the two resonances of methanol over a range of temperatures and correlating $\Delta\delta$ with known values. For NMR spectra exhibiting exchange broadening, rate constants for exchange were estimated with the DNMR3 spectral simulation program. Fourier-transform infrared spectra were recorded on a Mattson Galaxy Series 5000 instrument at 2 cm$^{-1}$ resolution. Elemental microanalyses were performed by Oneida Research Services, Inc.

X-ray diffraction data were collected with Mo Kα radiation, $\lambda = 0.710\,73$ Å. For **2a**, data were collected on an Enraf-Nonius CAD-4 diffractometer using the $\omega$ scan technique through a maximum $2\theta = 49.9°$, giving 6389 unique reflections of the 6842 collected. Cell dimensions were determined from 25 carefully centered reflections in the range $25.00° < 2\theta < 32.00°$ by least-squares analysis. Hydrogen

[⊗] Abstract published in *Advance ACS Abstracts,* April 1, 1997.

(1) (a) Thompson, M. S.; Meyer, T. J. *J. Am. Chem. Soc.* **1981**, *103*, 5577. (b) Murphy, W. R.; Takeuchi, K. J.; Barley, M. H.; Meyer, T. J. *Inorg. Chem.* **1986**, *25*, 1041. (c) Coia, G. M. Ph.D. Dissertation, University of North Carolina at Chapel Hill, 1996.

(2) Coia, G. M.; White, P. S.; Meyer, T. J.; Wink, D. A.; Keefer, L. K.; Davis, W. M. *J. Am. Chem. Soc.* **1994**, *116*, 3649.

S0020-1669(96)01025-7 CCC: $14.00 

atoms were included in the structure factor calculation in idealized positions (C−H = 0.95 A) and were assigned isotropic thermal parameters which were 20% greater than the $B_{eq}$ value of the atom to which they were bonded. The final cycle of full-matrix least-squares refinement was based on 4025 observed reflections of $I > 3.00\sigma(I)$ and 438 variable parameters. For **2c**, data were collected on a Rigaku diffractometer by using the $\theta/2\theta$ scan technique through a maximum $2\theta = 45°$, giving 4782 collected reflections, all of which were unique. Cell dimensions were determined from 25 reflections in the range $20.03° < 2\theta < 27.44°$ by least-squares analysis. The final least-squares cycle was calculated with 91 atoms, 418 parameters, and 3500 reflections of $I > 2.50\sigma(I)$. Prior to refinement, diffraction data were corrected for absorption of Mo Kα (linear absorption coefficient $\mu = 36.9$ cm$^{-1}$). For **2a** and **2c**, corrections for Lorentz and polarization effects were applied, as well as a correction for secondary extinction ($0.10 \times 10^{-6}$).

Resonance Raman spectra were obtained by use of an intensified charge coupled device (ICCD) detection system (Princeton Model 576G/RB) with an ST 130 detector controller interfaced to an 80386-based computer. Data were collected and processed with Princeton Instruments CSMA software. Laser excitation at 441.6 nm was provided by a Liconix Model 4240NB HeCd laser while excitation at 488 nm was provided by a Spectra-Physics 165 $Ar^+$ laser. Spectra were obtained from solutions which were millimolar in metal complex in NMR tubes with the laser beam focused onto the sample through a glass lens. The scattered light was collected with a 135° backscattering geometry by using a conventional camera lens and dispersion achieved with a SPEX 1877 triple spectrometer equipped with a 1200 groove/mm grating. The ICCD was calibrated to the known Raman bands of solvents.

Electrochemical measurements and preparative electrolyses were conducted by using a PAR Model 273 potentiostat. For voltammetry in aqueous solution, a glassy carbon disk working electrode and an SSCE reference electrode were used. For measurements in nonaqueous solution, the working electrode was a platinum disk, and the reference was a silver wire immersed in a $CH_3CN$ solution which was 0.01 M in $AgNO_3$ and 0.1 M in tetra-*n*-butylammonium hexafluorophosphate (TBAH). For cyclic voltammetry experiments employing scan rates greater than 2 V/s, an analog waveform generator (PAR Model 175) was used to supply the triangle wave to the potentiostat. The analog current and voltage outputs of the potentiostat were sampled by a Tektronix Model 2230 digital storage oscilloscope (100 MHz). Acetonitrile was distilled from calcium hydride prior to use in electrochemical experiments. TBAH was recrystallized three times from absolute ethanol and dried *in vacuo*. Buffers for aqueous voltammetry were prepared by neutralizing solutions of reagent A with solid or concentrated reagent B until the desired pH was reached. For pH 7.6−10.0, A = 0.3 M NaOH, B = $H_3BO_3$; for pH 5.8−7.8, A = 0.5 M $NaH_2PO_4$, B = NaOH; for pH 3.6−5.6, A = 0.5 M $CH_3COOH$, B = NaOH; for pH 2.2−3.8, A = 0.075 M potassium hydrogen phthalate, B = $H_2SO_4$; for pH 1−2.2, A = 0.5 M $Na_2SO_4$, B = $H_2SO_4$. Electrolytes of pH <1 consisted of solutions of $H_2SO_4$.

**Calculations.** Extended Hückel calculations were carried out by using the Personal CAChe application (CAChe Scientific) on a Macintosh Power PC. A basis contraction of STO-6G was employed, and a Wolfsberg−Helmholz constant of 1.75 was chosen. Standard atomic parameters from the set collected by Alvarez were used, which included for osmium $-H_{ss} = 8.17$ ($\zeta_{6s} = 2.429$), $-H_{pp} = 4.81$ ($\zeta_{6p} = 2.429$), and $-H_{dd} = 11.84$ ($\zeta_1 = 5.5710$, $c_1 = 0.6372$, $\zeta_2 = 5.5710$, $c_2 = 0.6372$).

**Preparations.** Amines were redistilled and stored under argon prior to use. Preparative electrolyses were conducted in a three-compartment cell with a platinum auxiliary electrode and an SSCE reference electrode. For oxidations, a reticulated vitreous carbon working electrode was used. For reductions, the working electrode was a mercury pool. Buffered electrolyte solutions were prepared by neutralizing 0.50 M aqueous solutions of the desired amine to pH 7.0 by addition of $NaH_2PO_4$. Electrolyte solutions and working electrodes were conditioned by electrolyzing exhaustively at the electrolysis potential prior to intoducing the complex to the cell. Cation exchange chromatography was conducted on Sephadex CM C-25 as the column support. Sparingly water soluble salts were dissolved in 9:1 water/acetonitrile mixtures to assist in loading. Pure products were precipitated by addition of $NH_4PF_6$ or $NaPF_6$ to the eluent. Stirring was maintained for 45 min at 0 °C before collection. The solids were then washed with ice-cold water followed by anhydrous diethyl ether. [Ru(bpy)$_3$](PF$_6$)$_3$ for use as a stoichiometric oxidant was prepared as described previously.[3]

**[Os(tpy)(bpy)(NH$_3$)](PF$_6$)$_2$ (1)** was prepared by using a modification of a published procedure.[1b] [Os(tpy)(bpy)(NO$_2$)](PF$_6$)[4] (1.25 g) was stirred in 100 mL of 0.2 M aqueous HCl and 10 mL of acetonitrile until both solid and solution became yellow, due to conversion of the nitro to the nitrosyl complex. The suspension was then stirred for 5 h with several pieces of freshly amalgamated zinc. After filtration and removal of the acetonitrile by rotary evaporation, 1 g of $NH_4PF_6$ was added, and the mixture was stirred at 0 °C for 1 h. The dark solid was collected by filtration and purified by cation exchange chromatography with 0.2 M $NH_4Cl$ as the eluent. $^1$H-NMR (200 MHz, acetone-$d_6$, 293 K): $\delta$/ppm = 3.79 (s, br, 3H, $NH_3$), 7.05 (t, 1H, $J$ = 6.2 Hz), 7.35−7.50 (m, 3H), 7.68 (q, 2H, J = 8.2 Hz), 7.85−8.20 (m, 6H), 8.61 (t, 3H, $J$ = 8.9 Hz), 8.76 (d, 2H, J = 7.9 Hz), 8.92 (d, 1H, $J$ = 7.6 Hz), 9.67 (d, 1H, J = 5.4 Hz).

**[Os(tpy)(bpy)(NNEt$_2$)](PF$_6$)$_3$ (3a).** A 1.75 mM solution of **1** in buffered diethylamine electrolyte was exhaustively oxidized at 0.65 V.[5] The color changed from brown to green and finally to amber, with 4.6−5.0 equiv of electrons consumed. The yellow product was precipitated by addition of $NH_4PF_6$, was redissolved in water, and was purified by cation exchange chromatography with 0.3 M $NH_4Cl$ as the eluent. Anal. Calcd/found: C, 31.64/31.70; N, 8.91/8.95; H, 2.66/2.63. $^1$H-NMR (200 MHz, $CD_3CN$, 293 K) revealed a series of broad features from +40 to −20 ppm.

**[Os(tpy)(bpy)(N$_2$)](PF$_6$)$_2$ (4).** In the dark, a 1.75 mM solution of **1** in buffered *n*-propylamine electrolyte was exhaustively oxidized at 0.65 V. The color changed from brown to pale red, with 5.2 equiv of electrons consumed. The red-brown product was precipitated by addition of $NaPF_6$ and purified by cation exchange chromatography with 0.2 M NaCl as the eluent. Anal. Calcd/found: C, 33.45/33.74; N, 10.93/10.09; H, 2.14/2.19. $^1$H-NMR (200 MHz, $CD_3CN$, 293 K) showed only pyridyl resonances: $\delta$/ppm = 7.13−7.23 (m, 2H), 7.41 (t, 2H), 7.74 (d, 2H), 7.84−7.97 (m, 2H), 8.03 (t, 2H), 8.15−8.29 (m, 2H), 8.35−8.45 (m, 3H), 8.60 (t, 3H), 9.46 (d, 1H).

**[Os(tpy)(bpy)(NNR$_2$)](PF$_6$)$_2$ (2).** The ammino complex of salt **1** was oxidized in buffered electrolyte solutions containing diethylamine, morpholine, and piperidine exactly as described above for the synthesis of [Os(tpy)(bpy)(NNEt$_2$)](PF$_6$)$_3$. However, when the current had decayed to a small value, the electrolysis potential was changed to 0.0 V and the solution was reduced exhaustively at this potential, with 1.0 equiv of electrons consumed based on the value of *n* obtained for the oxidation. The dark green products were precipitated by addition of $NH_4PF_6$ and were purified by cation exchange chromatography with 0.2 M $NH_4Cl$ as the eluent. Crystals suitable for X-ray diffraction were grown by vapor diffusion of diethyl ether into acetonitrile solutions of **2** at room temperature. The data for R$_2$ = Et$_2$ **(2a)** are as follows. Anal. Calcd/found: C, 36.45/36.54; N, 10.26/10.12; H, 3.06/3.04. $^1$H-NMR (200 MHz, $CD_3CN$, 293 K) revealed pyridyl resonances [$\delta$/ppm = 6.47 (d, 1H), 7.16 (t, 1H), 7.25 (t, 2H), 7.59 (t, 1H), 7.68 (d, 2H), 7.84 (m, 3H), 8.06 (t, 1H), 8.20 (t, 1H), 8.37 (d, 2H), 8.50 (t, 3H), 8.73 (d, 1H), 9.89 (d, 1H)], as well as two broad features corresponding to the diethyl protons [0.83 (br, 6H), 3.2 (v br, 4H)]. The data for R$_2$ = $(CH_2CH_2)_2CH_2$ **(2b)** are as follows. Anal. Calcd/found: C, 37.23/37.15; N, 10.13/10.03; H, 3.03/2.80. $^1$H-NMR (200 MHz, $CD_3CN$, 293 K) revealed pyridyl resonances [$\delta$/ppm = 6.49 (d, 1H), 7.16 (t, 1H), 7.26 (t, 2H), 7.59 (t, 1H), 7.69 (d, 2H), 7.86 (t, 2H), 8.05 (t, 1H), 8.24 (t, 1H), 8.37 (d, 2H), 8.49 (t, 3H), 8.74 (d, 1H), 9.90 (d, 1H)], as well as four broad features corresponding to the methylene protons [0.92 (br, 2H), 1.50 (br, 4H), 2.62 (br, 2H), 3.86 (br, 2H)]. The data for R$_2$ = $(CH_2CH_2)_2O$ **(2c)** are as follows. Anal. Calcd/found: C, 35.91/35.52; N, 10.11/9.86; H, 2.81/2.66. $^1$H-NMR (200 MHz, $CD_3CN$, 293 K) revealed pyridyl resonances [$\delta$/ppm = 6.49 (d, 1H), 7.18

(3) DeSimone, R. E.; Drago, R. S. *J. Am. Chem. Soc.* **1970**, *92*, 2343.
(4) Pipes, D. W.; Meyer, T. J. *Inorg. Chem.* **1984**, *23*, 2466.
(5) All potentials reported here are referenced to the saturated NaCl calomel electrode (SSCE) and are measured to ±5 mV. Potentials for irreversible processes are subject to greater error and are reported to two decimal places.

(t, 1H), 7.27 (t, 2H), 7.61 (t, 1H), 7.68 (d, 2H), 7.88 (t/m, 3H), 8.04 (t, 1H), 8.25 (t, 1H), 8.37 (d, 2H), 8.45−8.56 (m, 3H), 8.74 (d, 1H), 9.91 (d, 1H)], as well as four broad features corresponding to the methylene protons [2.58 (br, 2H), 3.07 (br, 2H), 3.62 (br, 2H), 3.85 (br, 2H)].

**$[Os(tpy)(bpy)(NNR_2)](PF_6)_3$.** Complex **3a** was purified by cation exchange chromatography without complication. **3b** and **3c** were more conveniently prepared by electrochemical oxidation of the prepurified salts of **2**. In general, a 3−5 mM solution of $[Os(tpy)(bpy)(NNR_2)](PF_6)_2$ in acetonitrile containing 0.1 M TBAH was exhaustively oxidized at 0.90 V. The color changed from green to amber, while 1.0 equiv of electrons was consumed. The anolyte was withdrawn from the cell and taken to dryness by rotary evaporation. The residue was twice suspended in rapidly stirring dichloromethane for 30 min, and the dichloromethane washings were discarded. The yellow or yellow-orange solid was collected by filtration and washed with dichloromethane followed by diethyl ether. The data for $R_2 = (CH_2CH_2)_2CH_2$ **(3b)** are as follows. Anal. Calcd/found: C, 32.38/31.94; N, 8.81/8.70; H, 2.63/2.51. The data for $R_2 = (CH_2CH_2)_2O$ **(3c)** are as follows. Anal. Calcd/found: C, 31.24/30.81; N, 8.80/8.56; H, 2.45/2.40. $^1$H-NMR (200 MHz, $CD_3CN$, 293 K) revealed broad features from +40 to −20 ppm.

## Results

**Synthesis.** Detailed electrochemical measurements on **1** and the analogous ruthenium complex have suggested that a highly electrophilic $Os^{IV}$ species is generated by rapid disproportionation of the $Os^{III}$ ammine (eq 2), which is spontaneous above pH 4.[1] In aqueous solutions where added nucleophiles are

$$2[Os(tpy)(bpy)(NH_3)]^{3+} \rightarrow [Os(tpy)(bpy)(NH_3)]^{2+} + [Os(tpy)(bpy)(NH)]^{2+} + 2H^+ \quad (2)$$

absent, the $Os^{IV}$ species further disproportionates, resulting ultimately in the appearance of $[Os(tpy)(bpy)(NH_3)]^{2+}$ and $[Os(tpy)(bpy)(NO)]^{3+}$, the six-electron oxidation product.

$$3[Os(tpy)(bpy)(NH)]^{2+} + H_3O^+ \rightarrow 2[Os(tpy)(bpy)(NH_3)]^{2+} + [Os(tpy)(bpy)(NO)]^{3+} \quad (3)$$

Exhaustive oxidation of **1** above pH 4.5 occurs by loss of six electrons and gives the nitrosyl as the exclusive product.

In aqueous solutions containing high (0.5 M) concentrations of secondary ammonium salts, oxidation of **1** afforded terminal hydrazides of osmium, *formally* in oxidation state V. This is consistent with a step in which nucleophilic attack on the $Os^{IV}$ intermediate by the amine occurs. The amine is present at pH 7 in small, equilibrium amounts.

$$[Os(tpy)(bpy)(NH)]^{2+} + NHR_2 \rightarrow [Os(tpy)(bpy)NH_2NR_2]^{2+} \quad (4)$$

At the applied electrolysis potential (0.65 V), the hydrazine complex undergoes further oxidation (eq 5). Experimentally, 4.6−5.0 equiv of electrons is consumed per equivalent of starting complex.

$$[Os(tpy)(bpy)NH_2NR_2]^{2+} \xrightarrow{-2H^+/3e^-} [Os(tpy)(bpy)(NNR_2)]^{3+} \quad (5)$$

Electrochemical reduction of solutions of $[Os(tpy)(bpy)(NNR_2)]^{3+}$ **(3)**, in both aqueous and nonaqueous electrolytes, occurred with $n = 1.0$ (eq 6). From the catholyte solutions, *formally* $Os^{IV}$ products **(2)** were precipitated. These salts were

$$[Os(tpy)(bpy)(NNR_2)]^{3+} \xrightarrow{+e^-} [Os(tpy)(bpy)(NNR_2)]^{2+} \quad (6)$$

purified by cation exchange chromatography. This method of purification was also suitable for **3a**. More generally, **3** was prepared in pure form by oxidation of the corresponding, prepurified salt of **2** in nonaqueous electrolyte solutions.

When the electrolysis was conducted in the presence of primary ammonium salts or $NH_4^+$, the likely first product was again the $Os^{II}$ hydrazine complex.

$$[Os(tpy)(bpy)(NH)]^{2+} + NH_2R \rightarrow [Os(tpy)(bpy)NH_2NHR]^{2+} \quad (7)$$

R = alkyl group or H atom

Subsequent oxidation of the hydrazine afforded a terminal dinitrogen complex, possibly *via* carbocation (or proton) loss from an unstable diazonium intermediate (eqs 8 and 9).

$$[Os^{II}(tpy)(bpy)NH_2NHR]^{2+} \xrightarrow{-3H^+/4e^-} [Os(tpy)(bpy)(NNR)]^{3+} \quad (8)$$

$$[Os(tpy)(bpy)(NNR)]^{3+} \rightarrow [Os^{II}(tpy)(bpy)(N_2)]^{2+} + R^+ \quad (9)$$

Coulometry was used to verify that 5.9−6.3 equiv of electrons were consumed per equivalent of starting complex. Although the dinitrogen complex was identified as the major product of electrolysis with either $NH_3R^+$ or $NH_4^+$ in the electrolyte, the yield was typically higher when primary ammonium salts were used. This may be due to the greater nucleophilicity of $NH_2R$ over $NH_3$ contributing to a faster net reaction. In the slower reaction with $NH_3$, significant decomposition of the product occurred before it was isolated (*vide infra*).

The results of two failed synthetic attempts are mechanistically revealing. Bulk oxidation of **1** in buffered triethylamine solution resulted in quantitative formation of $[Os(tpy)(bpy)(NO)]^{3+}$. The product solution was the same as that obtained when the electrolysis was conducted in the absence of trapping agents ($NaH_2PO_4/Na_2HPO_4$ buffer). By coulometry, the electron count was 5.9 ± 0.2 electrons.

We attempted to generate the hydrazido complexes directly from $[Os(tpy)(bpy)(NO)]^{3+}$. In previous work, it was shown that ruthenium nitrosyl species promote the azotization and nitrosation of aromatic amines.[6] However, at least under conditions relevant to our study, $[Os(tpy)(bpy)(NO)]^{3+}$ showed no reactivity toward any of the buffered amine solutions used in the trapping experiments. In some cases, a very slow reaction was observed, generating small amounts of **1** over a period of many hours.

**$^1$H-NMR Spectroscopy.** Salts of **2** are diamagnetic, exhibiting sharp pyridyl signals in the $^1$H-NMR, but resonances attributed to the aminoalkyl protons are broad at room temperature. Broadness is attributed to *near-fast* exchange of the alkyl groups caused by rotation about the N−N axis. At 238 K and below, the exchange is blocked and the alkyl groups are fully inequivalent. Rate constants for exchange were estimated for each spectrum of **2a** recorded in the intermediate exchange region (238−298 K), and kinetic parameters were obtained from the Eyring plot, which gave $\Delta S^{\ddagger} = 52.3$ J mol$^{-1}$ K$^{-1}$, $\Delta H^{\ddagger} = 71.5$ kJ mol$^{-1}$, and $\Delta G^{\ddagger} = 55.9$ kJ mol$^{-1}$ at 298 K. In strongly acidic solutions, where **2** are fully protonated, the alkyl groups are inequivalent even at room temperature: the hydrazido(1−) form of the complex exhibits a higher rotational barrier.

(6) (a) Bowden, W. L.; Little, W. F.; Meyer, T. J. *J. Am. Chem. Soc.* **1976**, *98*, 444. (b) Bowden, W. L.; Little, W. F.; Meyer, T. J. *J. Am. Chem. Soc.*, **1977**, *99*, 4340.

**Table 1.** Crystallographic Details and Collection and Refinement Parameters

| | **2a** | **2c** |
|---|---|---|
| empirical formula | $C_{31}H_{32}N_8F_{12}P_2Os$ | $C_{31}H_{30}N_8O_1F_{12}P_2Os$ |
| formula wt | 996.78 | 1010.75 |
| system | triclinic | triclinic |
| space group | $P\bar{1}$ | $P\bar{1}$ |
| *a*, Å | 9.004(1) | 9.632(8) |
| *b*, Å | 9.796(1) | 21.229(9) |
| *c*, Å | 20.710(2) | 9.039(5) |
| α, deg | 88.78(2) | 97.41(4) |
| *β*, deg | 85.43(2) | 94.28(5) |
| *γ*, deg | 86.22(2) | 85.07(5) |
| *V*, Å$^3$ | 1816.7(7) | 1822.2(20) |
| *Z* | 2 | 2 |
| *T*/, °C | 23 | 20 |
| $\mu$ (mm$^{-1}$), $\lambda$ (Å) | 3.689, 0.710 69 | 3.68, 0.709 30 |
| $D_{calc}$, g cm$^{-3}$ | 1.749 | 1.842 |
| $R^a$ | 0.068 | 0.079 |
| $R_w{}^a$ | 0.075 | 0.105 |
| GOF$^a$ | 1.69 | 1.39 |
| max resd, e$^-$/Å$^3$ | 2.08 | 3.07 |
| min resd. e$^-$/Å$^3$ | −1.87 | −2.35 |

$^a$ $R = \sum(|F_o| - |F_c|)/\sum|F_o|$; $R_w = [\sum w(F_o - F_c)^2/\sum wF_o|^2]^{1/2}$; GOF $= [\sum w(F_o - F_c)^2/(n_{rflns} - n_{params})]^{1/2}$.

**Table 2.** Bond Lengths (Å) and Bond Angles (deg) for Hydrazido(2−) Complexes

| | 2a | 2c |
|---|---|---|
| Os−NA | 1.89(1) | 1.849(16) |
| Os−N1 | 2.06(1) | 2.000(15) |
| Os−N2 | 1.95(1) | 1.979(15) |
| Os−N3 | 2.06(1) | 2.082(13) |
| Os−N4 | 2.14(1) | 2.115(14) |
| Os−N5 | 2.05(1) | 1.975(23) |
| NA−NB | 1.25(2) | 1.405(24) |
| NB−C1 | 1.54(2) | 1.52(3) |
| NB−C3 | 1.48(2) | 1.40(3) |
| N1−Os−N3 | 157.6(5) | 156.7(5) |
| N4−Os−N5 | 75.3(6) | 79.0(6) |
| Os−NA−NB | 137(1) | 137.1(12) |
| NA−NB−C1 | 119(1) | 118.9(18) |
| NA−NB−C3 | 129(1) | 126.8(16) |
| C1−NB−C3 | 113(1) | 113.3(18) |

Resonances of odd-electron **3** are contact-shifted to a range of *ca.* 60 ppm; all peaks exhibit severe paramagnetic broadening.

The dinitrogen complex is diamagnetic on the basis of $^1$H-NMR. Evidence for solvolysis is found in both the NMR and UV−visible spectra, with $t_{1/2} = 8.0$ h in acetonitrile at 298 K. Solvolysis is greatly accelerated in the presence of visible light, but this effect was not studied in detail. Loss of $N_2$ occurred also in the solid state, as indicated by spectral changes which took place over a period of days even when the complex was stored in the dark under dry conditions.

**X-ray Crystallography.** Parameters relating to the solution and refinement of the structures of **2a** and **2c** are summarized in Table 1, while the more relevant metrical data are given in Table 2. For **2a**, one of the anions failed to refine adequately and was subjected to subsequent refinement as a rigid group with assigned isotropic thermal parameters to each atom. For **2c**, both $PF_6^-$ ions were disordered. One of them showed no difference peaks and was treated normally. The other was modeled by two superimposed rigid bodies, each with approximately 50% occupancy. Both compounds crystallized with one $CH_3CN$ of solvation per molecule. The structures of the cations are illustrated in Figure 1.

**Electrochemistry in Acetonitrile.** For clarity, redox couples are labeled according to the formalism in which the hydrazido ligand is a dianion, $NNR_2^{2-}$. The formal oxidation state of the metal is IV in **2** and V in **3**, so the couple which relates them is written Os(V/IV). In later sections the relevancy of this formalism is discussed.

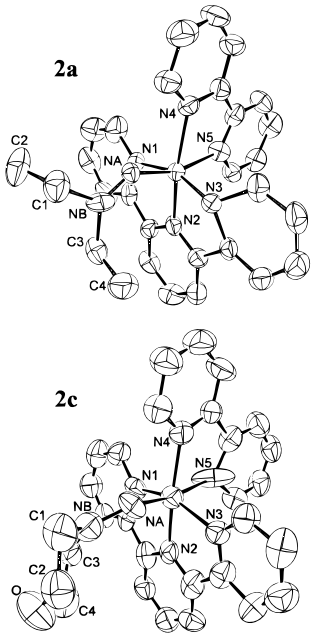


**Figure 1.** ORTEP representations (50% probability ellipsoids) of the cations in **2a** and **2c**, as determined by X-ray crystallography. The scale is the same for both structures.

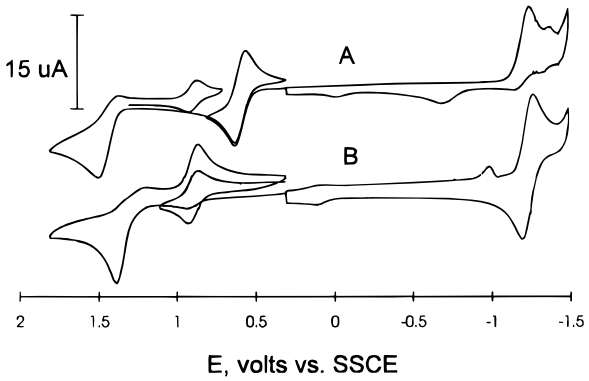


**Figure 2.** Cyclic voltammograms recorded in $CH_3CN$ solutions 0.1 M in TBAH. The scan rate is 50 mV/s: (A) $[Os(tpy)(bpy)(NNEt_2)](PF_6)_2$ **(2a)**; (B) $[Os(tpy)(bpy)(N_2)](PF_6)_2$ **(4)**. Small waves at +0.10 and −0.95 V are due to impurities which developed subsequent to the chromatography.

Cyclic voltammetry of complexes **2** and **3** reveals reversible Os(V/IV) waves and quasireversible or irreversible Os(VI/V) waves. A representative cyclic voltammogram is shown in Figure 2A. The measured reduction potentials in Table 3 demonstrate that $E_{1/2}$ for the Os(V/IV) couple is strongly influenced by the $NR_2$ moiety. Coulometric oxidation of **2** and reduction of **3** (in all cases) establish the electron count for this process to be unity.

$$[Os(tpy)(bpy)(NNR_2)]^{2+} \underset{+e^-}{\overset{-e^-}{\rightleftharpoons}} [Os(tpy)(bpy)(NNR_2)]^{3+} \quad (10)$$

At sufficiently high scan rates, the next stage of oxidation is one-electron and reversible for all of the hydrazido complexes, but as the scan rate is decreased, the cathodic component diminishes in peak current, and a new wave corresponding to $[Os(tpy)(bpy)(NCCH_3)]^{3+/2+}$ grows in. This was determined by comparison of the $E_{1/2}$ value of the reversible product wave

**Table 3.** Reduction Potentials for Hydrazido(2−) Complexes

| | | $E_{1/2}$, V | | | |
|---|---|---|---|---|---|
| | | Os(V/IV) | | Os(VI/V) | |
| salt | couple | $CH_3CN$[a] | $H_2O$[b] | $CH_3CN$[a] | $H_2O$[b] |
| **2a** | $[Os(tpy)(bpy)(NNEt_2)]^{3+/2+}$ | +0.586 | +0.360 | +1.425 | +1.18[c] |
| **2b** | $[Os(tpy)(bpy)(NN(CH_2)_2CH_2)]^{3+/2+}$ | +0.625 | +0.397 | +1.415 | +1.16[c] |
| **2c** | $[Os(tpy)(bpy)(NN(CH_2)_2O)]^{3+/2+}$ | +0.669 | +0.464 | +1.489 | +1.22[c] |

[a] 0.1 M in TBAH. [b] 0.5 M in $PO_4$, pH 7.0. [c] Irreversible oxidation. $E_{pa}$ value is given.

with the Os(III/II) potential of the acetonitrile complex, measured in the same electrolyte solution: $E_{1/2} = +0.891$ V. At a scan rate of 100 mV/s, the Os(V/IV) wave is quasireversible for **2b**/**3b** and **2c**/**3c** and irreversible for **2a**/**3a**. Peak height comparison suggests that the oxidation is a one-electron process, even at slow scan rates, where the return wave is absent. However, exhaustive bulk oxidation at potentials just anodic of the wave indicate that *ca.* 3 equiv of electrons is consumed. The exclusive electroactive product of the oxidation is $[Os(tpy)(bpy)(NCCH_3)]^{3+}$. These observations clearly argue for an EC mechanism with reversible, one-electron transfer as the first step.

$$[Os(tpy)(bpy)(NNR_2)]^{3+} \underset{+e^-}{\overset{-e^-}{\rightleftharpoons}} [Os(tpy)(bpy)(NNR_2)]^{4+} \quad (11)$$

$$[Os(tpy)(bpy)(NNR_2)]^{4+} \rightarrow [Os(tpy)(bpy)(NCCH_3)]^{3+} + \text{products} \quad (12)$$

By analysis of anodic and cathodic peak heights of the Os(VI/V) wave as a function of scan rate, the rate constants of decomposition of $[Os^{VI}(tpy)(bpy)(NNR_2)]^{4+}$ were estimated.[7] For the decomposition of $[Os(tpy)(bpy)(NNEt_2)]^{4+}$ (derived from **2a**), $k = 8.10 \pm 0.10\ s^{-1}$. The analogous piperidide adduct (from **2b**) decomposes more slowly: $k = 0.200 \pm 0.005\ s^{-1}$. The relevant conditions are $T = 298$ K, in acetonitrile 0.1 M in TBAH. The rate of decomposition of the morpholide adduct (from **2c**) is too slow to be accurately measured by cyclic voltammetry ($k < 0.03\ s^{-1}$).[8]

In dry acetonitrile, several irreversible reductive waves were observed for each of the hydrazido complexes (e.g., $E_{pc} = -1.23, -1.38, -1.55, -1.80$ V, for **2a**), but detailed investigation of the reductive electrochemistry was confined to aqueous solution, where the proton composition of the electrolyte could be readily controlled.

A cyclic voltammogram of $[Os(tpy)(bpy)(N_2)]^{2+}$ is shown in Figure 2B. Oxidation to $Os^{III}$ occurred irreversibly at $E_{pa} = +1.39$ V and resulted in loss of dinitrogen. Subsequent coordination of acetonitrile was indicated by the presence of a new, reversible wave at $E_{1/2} = +0.894$ V following the oxidative scan.

$$[Os(tpy)(bpy)(N_2)]^{2+} \xrightarrow{-e^-} [Os(tpy)(bpy)(N_2)]^{3+} \xrightarrow{CH_3CN} N_2 + [Os(tpy)(bpy)(NCCH_3)]^{3+} \quad (13)$$

**Chemical Oxidation of Hydrazido.** $[Os(tpy)(bpy)(NNR_2)](PF_6)_2$ (**2**) reacts instantly with $[Ru(bpy)_3](PF_6)_3$ in $CD_3CN$ solution at 25 °C. When 2 equiv of the ruthenium complex was added to **2a**, the products $[Ru(bpy)_3]^{2+}$ and $C_2H_5NHCOCD_3$ were observed by $^1$H-NMR and $[Os(tpy)(bpy)(NCCH_3)]^{3+}$, which is paramagnetic with broad resonances over an extended chemical shift range, by cyclic voltammetry. The acetamide was the only product by NMR.

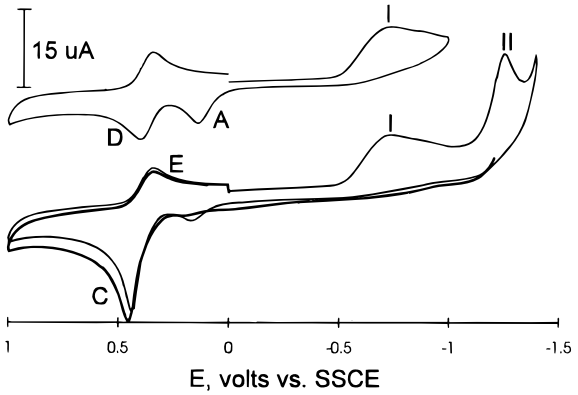


**Figure 3.** Cyclic voltammograms of $[Os(tpy)(bpy)(NNEt_2)](PF_6)_2$ **(2a)** recorded at pH 8.0 with a scan rate of 100 mV/s. The heavy line shows the effect of holding the potential for 30 s at the reductive limit prior to execution of the scan.

**Electrochemistry in Aqueous Solution.** The oxidative electrochemistries of the osmium hydrazido and dinitrogen complexes were similar in aqueous solution and in acetonitrile. In each case, however, the Os(VI/V) wave was totally irreversible at ordinary scan rates. Oxidation ($E_{pa} = +1.14$ V for **4**, *cf.* Table 3) of compounds **2**−**4** again afforded the $Os^{III}$ solvento, in this case $[Os(tpy)(bpy)(H_2O)]^{3+}$, as confirmed by its pH-dependent electrochemistry.[9]

Reduction of **2** occurs in two stages, as shown by the pair of irreversible, cathodic waves in the cyclic voltammetry. Both waves are present in aqueous solutions above pH 4, below which the reduction of protons begins to obscure the second wave. The products which emerge following reduction through each of these waves are different, as shown by the cyclic voltammograms in Figure 3 at pH 8.0. Reduction through wave II generates **1**, as determined by comparison of $E_{pa}$ values with an authentic sample (Scheme 1). Reduction just past wave I generates none of the ammino complex, but instead gives an intermediate whose irreversible reoxidation occurs at $E_{pa} = +0.14$ V (wave A). By extending the anodic scan through wave D it is evident that the starting complex of **2** has been regenerated. We postulate that the intermediate produced at wave I and oxidized at wave A is the hydrazine complex $[Os(tpy)(bpy)(NH_2NR_2)]^{2+}$ (eq 14) and that its oxidation regenerates the hydrazido. The second reductive feature (wave II) corresponds to reduction of the hydrazine complex by two electrons.

$$[Os(tpy)(bpy)(NNR_2)]^{2+} \xrightarrow{+2H^+/2e^-} [Os(tpy)(bpy)(NH_2NR_2)]^{2+} \quad (14)$$

(7) Nicholson, R. S.; Shain, I. *Anal. Chem.* **1964**, *36*, 706. The appropriate working curve appears in Table IX of this reference.

(8) Based on the observation that, at 100 mV/s, $i_{pc}/i_{pa} > 0.90$. To reach desirable ratios the scan rate would have to be less than 25 mV/s, where convective effects become important.

(9) Pipes, D. W.; Meyer, T. J. *Inorg. Chem.* **1986**, *25*, 4042.

**Scheme 1.** Reactions of Hydrazido(2−) Complexes[a]

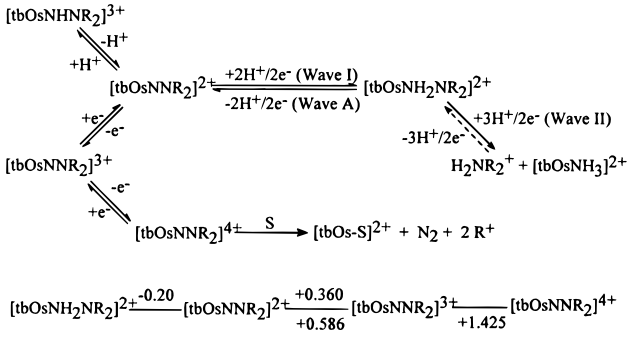


[a] t = tpy; b = bpy. The dashed line indicates that the process may be reversible only in the presence of high concentrations of the amine. Potentials above the line on the Latimer diagram are measured in aqueous solution, pH 7.0; potentials below the line are measured in $CH_3CN$, 0.1 M in TBAH. All potentials are *vs* SSCE.

$$[Os(tpy)(bpy)(NH_2NR_2)]^{2+} \xrightarrow{+3H^+/2e^-} [Os(tpy)(bpy)(NH_3)]^{2+} + H_2NR_2^+ \quad (15)$$

Waves I, II, and A are observed through an extended pH range, but only in basic solutions (pH >7) is the cyclic voltammetry uncomplicated by the homogeneous decomposition of $[Os(tpy)(bpy)(NH_2NR_2)]^{2+}$. In neutral and acidic solutions, reduction through wave II gives the ammino complex, but the distribution of products following reduction through wave I is a function of the pH and the scan rate. Voltammograms of **2a** were recorded at several different scan rates in solutions of pH 5.0. (These appear in the Supporting Information.) Below pH 6, wave A is observed only at higher scan rates because decomposition of the hydrazine complex has become rapid on the cyclic voltammetry time scale. This process results in the appearance of **1** following reduction through wave I, and also in the enhancement of the peak current for wave I at the expense of wave II. Accordingly, the products of bulk reduction past the first reductive wave depend on the pH. In neutral and basic solutions, reduction gives **1** and an additional product, which is believed to be the hydrazine complex. However, at pH = 0.5, the reduction occurs with $n = 4.0 \pm 0.2$. Under these conditions, **1** is obtained quantitatively.

$$[Os(tpy)(bpy)(NNR_2)]^{2+} \xrightarrow{+5H^+/4e^-} [Os(tpy)(bpy)(NH_3)]^{2+} + NH_2R_2^+ \quad (16)$$

**Hydrazine Complex.** Decomposition of $[Os(tpy)(bpy)(NH_2NEt_2)]^{2+}$, generated by electrochemical reduction of $[Os(tpy)(bpy)(NNEt_2)]^{2+}$ in basic solution, was studied spectrophotometrically over an extended pH range. Addition of acid (to pH ~7) resulted in a color change, which was complete in 30 min. Precipitation of the products, followed by cation exchange chromatography, revealed that the osmium product was partitioned into equal amounts of **1** and **2a**.

$$[Os(tpy)(bpy)(NH_2NEt_2)]^{2+} \rightarrow [Os(tpy)(bpy)(NNR_2)]^{2+} + [Os(tpy)(bpy)(NH_3)]^{2+} + NH_2R_2^+ \quad (17)$$

Throughout pH 1−10, the stoichiometry of eq 15 was preserved, as determined by UV−visible spectroscopy. The reaction is characterized by isosbestic points at 310, 344, 450, 520, 692, and 804 nm, which are not sensitive to the pH. In solutions buffered to pH 7.7 and below, the reaction was first-order in osmium. In this region, $k_{obs}$ was also first-order in $[H^+]$. From the data in the first three entries of Table 4, a second-order rate constant of 220 $M^{-1}$ $s^{-1}$ was estimated. At higher pH, significant deviation from first-order kinetics occurred, with a gradual decrease in reaction order with respect to osmium as the solution became more basic. By pH 9.58, the reaction exhibited zero-order kinetics and was accurately fitted to the Michaelis−Menten equation (footnote *b*, Table 4). In the first-order domain, neither the stoichiometry nor the rate was affected by diethylamine present in large excess. At higher pH, the rate was significantly supressed in the presence of diethylamine, where the observed kinetics were first-order with respect to osmium, but the stoichiometry remained unaffected.

**Table 4.** Kinetic Data for the Decomposition of $[Os(tpy)(bpy)(NH_2NEt_2)]^{2+}$ in Aqueous Solution

| pH | [Os], $\mu$M | [$NHEt_2$], M | $k_{obs}$, $s^{-1}$ [a] |
|---|---|---|---|
| 6.77 | 35.2 | 0 | 23.4 |
| 7.40 | 25.7 | 0 | 6.19 |
| 7.65 | 47.7 | 0 | 3.25 |
| 7.65 | 43.4 | 0.05 | 3.21 |
| 8.38 | 48.1 | 0 | |
| 8.80 | 60.9 | 0 | |
| 9.58 | 63.3 | 0 | *b* |
| 9.58 | 55.5 | 0.05 | 0.00480 |

[a] $k_{obs}$ reported for runs obeying first-order kinetics. [b] Fit to the Michaelis−Menten equation, $-d[S]/dt = k[S]/(K_S + [S])$, $k = 2.5 \times 10^{-9}$ $s^{-1}$, $K_S = 1.5 \times 10^{-5}$ M, with [S] representing the concentration of $[Os(tpy)(bpy)(NH_2NEt_2)]^{2+}$.

**Hydrazido(1−) Complexes.** It has been shown that hydrazido(2−) complexes, including those of the bent geometry, can be protonated or alkylated at $N_\alpha$ to give hydrazido(1−) complexes.[10,11] Accordingly, **2** reacts instantly with strong anhydrous acids in aprotic solvents to give bright yellow solutions.

$$[Os(tpy)(bpy)(NNR_2)]^{2+} + H^+ \rightleftharpoons [Os(tpy)(bpy)(NHNR_2)]^{3+} \quad (18)$$

Cyclic voltammetry of a solution of **2a** to which a drop of $HBF_4 \cdot Et_2O$ was added (Supporting Information) demonstrates the disappearance of the reversible oxidation wave. For the hydrazido(1−) species, the first oxidation, which is irreversible, occurs at a potential slightly higher than the Os(VI/V) wave of hydrazido(2−). Oxidation through this wave leads to the solvento complex. The effect on the electronic absorption spectrum is shown in Figure 4; the effect on the $^1$H-NMR specturm was mentioned earlier. The original spectra and voltammograms were recovered on addition of excess $NaHCO_3$. Spectrophotometric titration of **2a** in aqueous solution indicates that its p$K_a$ is 0.90 ± 0.01. Similar spectral changes were observed when small amounts of other potent electrophiles (triethyloxonium tetrafluoroborate, acetyl bromide) were added to solutions of **2**. Regrettably, we have not been able to isolate any of the resulting hydrazido(1−) products in pure form.

**Vibrational Spectroscopy.** The infrared absorption spectrum of **4** exhibits a very strong band at 2148 $cm^{-1}$ both in KBr and in acetonitrile solution, which corresponds to $\nu_{NN}$. By comparing infrared and resonance Raman spectra of the series of hydrazido complexes with those of $[Os(tpy)(bpy)(L)](PF_6)_2$ (L = $NH_3$, $CH_3CN$) and $[Os(tpy)(bpy)(NO)](PF_6)_3$ as models, it was possible to identify bands which have their origins in the $NNR_2$ ligands or which arise from coupling of $NNR_2$ modes

(10) Chatt, J.; Dilworth, J. R.; Dahlstrom, P.; Zubieta, J. A. *J. Chem. Soc., Chem. Commun.* **1986**, 786.
(11) Barrientos-Penna, C. F.; Einstein, F. W. B.; Jones, T.; Sutton, D. *Inorg. Chem.* **1982**, *21*, 2578.

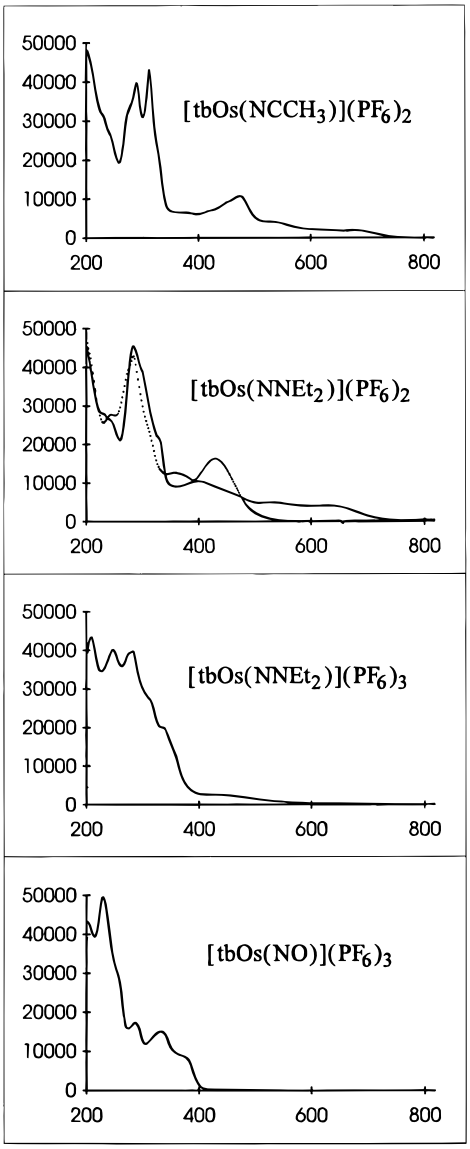


**Figure 4.** Comparison of the effects of various ligands on the electronic absorption spectra of $Os^{II}$(tpy)(bpy) complexes. The dashed curve is a spectrum recorded in 6.0 M aqueous HCl. For all other spectra, the solvent was $CH_3CN$. The vertical axis is $\epsilon$ in $M^{-1}$ $cm^{-1}$ and the horizontal axis $\lambda$ in nm.

with pyridyl modes. Hydrazido(2−) salts **2** and **3** were studied by IR spectroscopy as suspensions in KBr. The protonated [hydrazido(1−)] forms were studied by resonance Raman in strongly acidic solutions.

A resonance Raman spectrum of **2a** was recorded in 6.0 M aqueous HCl (Supporting Information). Under these conditions, >99% of the complex exists in the protonated, hydrazido(1−) form. Upon excitation at 441.6 nm, the most intense features are a pair of bands ($\nu_1$, $\nu_2$) at 698 and 755 $cm^{-1}$ and a weaker one at 821 $cm^{-1}$. The same pattern of bands is observed for solutions of **2b** and **2c** in this medium, with $\nu_2$ and $\nu_3$ shifted in position, as shown in Table 5.

Spectra of the same salts were recorded in 6.0 M DCl/$D_2O$. The resulting shifts in band positions are listed in Table 6. On the basis of the large values of the isotopic shifts for $\nu_1$ and $\nu_2$, it is likely that these bands correspond to vibrational modes which involve significant displacement at $N_\alpha$. The frequency of $\nu_2$ is quite sensitive to the alkyl substituents at $N_\beta$ and shifts ~10 $cm^{-1}$ lower in the deuteriated complex. The $\nu_3$ band is also sensitive to the substituents at $N_\beta$. While its frequency does not shift appreciably in the deuteriated solvent,

**Table 5.** Observed Band Positions ($cm^{-1}$) from Resonance-Raman Spectra of Hydrazido(1−) Complexes in 6.0 M HCl or DCl ($\lambda_{ex}$ = 441.6 nm)

| complex/solvent | $\nu_1$ | $\nu_2$ | $\nu_3$ | $2\nu_1$ | $\nu_1 + \nu_2$ |
|---|---|---|---|---|---|
| **2a**/HCl | 698 | 755 | 821 | 1398 | 1452 |
| **2a**/DCl | 672 | 745 | 842[b] | 1344[a] | 1419 |
| **2b**/HCl | 700 | 774 | 842 | 1397 | 1475 |
| **2b**/DCl | 671 | 762 | 842[b] | 1340 | 1431 |
| **2c**/HCl | 699 | 781 | 855 | 1398 | 1477 |
| **2c**/DCl | 673 | 771 | 860[b] | 1343 | 1439[a] |

[a] Incompletely resolved due to overlap with another band. Calculated value is given. [b] Weak relative to its intensity in the protonated complex.

**Table 6.** Observed and Calculated Isotopic Shifts ($cm^{-1}$) for Resonance-Raman Bands in Table 5

| complex | $\Delta\nu_1$(obs)[a] | $\Delta\nu_1$(calc)[b] | $\Delta\nu_2$(obs)[a] | $\Delta\nu_3$(obs)[a] |
|---|---|---|---|---|
| **2a** | −26 | −21 | −10 | −4 |
| **2b** | −29 | −21 | −12 | 0 |
| **2c** | −26 | −21 | −10 | +5 |

[a] $\Delta\nu = \nu$(DCl) − $\nu$(HCl). [b] Calculated for a pure Os−NH stretch based on reduced mass of NH *vs* ND.

**Table 7.** Observed Band Positions ($cm^{-1}$) from Infrared Spectra of Hydrazido(2−) Complexes in KBr

| $Os^{IV}$ complex | $\nu_{NN}$ | $Os^{V}$ complex | $\nu_{NN}$ |
|---|---|---|---|
| **2a** | 1259 | **3a** | 1332 |
| **2b** | 1234 | **3b** | 1349 |
| **2c** | 1219 | **3c** | 1340 |

its intensity decreases significantly. The $\nu_1$ band is rather insensitive to substituents at $N_\beta$, but exhibits a large isotopic shift in each case. The shift is greater than calculated for an Os−$N_\alpha$ stretch coupled to no other mode.

The degree of resonance enhancement of $\nu_1$ and $\nu_2$ with excitation into the MLCT absorption at 441.6 nm is remarkable. The integrated intensity of $\nu_1$ in each complex is about 20 times that for the band at 1608 $cm^{-1}$, a strong, polypyridyl-based band which appears in all $Os^{II}$(tpy)(bpy) complexes. This suggests that, for these modes, there is a considerable change in equilibrium displacement between ground and excited states.

We are not able to assign these bands definitively, but on the basis of their large isotopic shifts and strong resonance enhancements, they are likely to involve Os−$N_\alpha$ stretching, or in-plane or out-of-plane bending of the Os−$N_\alpha$−$N_\beta$ unit. Coupling to other local coordinates gives rise to $\nu_1$, which exhibits minimal displacement of atoms except the $N_\alpha$H group, and $\nu_2$, which involves displacement of the entire $NHNR_2$ group.

Strong overtone and combination bands are observed at $2\nu_1$ and $\nu_1 + \nu_2$. These are the most intense features in the 1200−1500 $cm^{-1}$ region, where N−N stretching bands for hydrazido ligands in other complexes have been reported. All other bands observed in this region have their origins in the polypyridyl ligands. A pair of weak bands between 1215 and 1275 $cm^{-1}$ show marked intensity variations depending on whether $N_\alpha$ is protonated or deuteriated. This points to some degree of coupling of the pyridyl-based modes with $N_\alpha$−H. It is significant that no band in the spectra could be identified as an N−N stretch.

The infrared spectrum of **2** suspended in KBr does show a strong band which is not present in the model complexes and which is sensitive to the substituents at $N_\beta$. Its position makes it a likely candidate for $\nu_{NN}$. This band disappears in the oxidized form (**3**); it reappears *ca.* 100 $cm^{-1}$ higher in frequency and again shows a dependence on the nature of R, Table 7.

Values of $\nu_{NN}$ in the range 1315−1510 $cm^{-1}$ have been obtained in the IR spectra of other hydrazido(2−) complexes,[12] although a comparison is not completely apt since there are no stretching frequencies reported for *bent* hydrazido complexes.

## Discussion

Investigations of the reactivity of very electrophilic imido (or nitrene) complexes began with Basolo's experiments on the decomposition of transition metal azides.[13]

$$[M(NH_3)_5(N_3)]^{2+} + H^+ \rightarrow [M(NH_3)_5(NH)]^{3+} + N_2 \quad (19)$$

$$M = Ru, Ir$$

Since that time, there have been few well-characterized examples of electrophilic $NH^{2-}$ complexes,[14] in contrast to the myriad of examples (found mainly in the chemistries of the earlier, more electron rich transition metals) in which the nitrogen is nucleophilic.[15]

It appears that eq 4 is the first example of the formation of a hydrazine complex by nucleophilic attack of a secondary amine on an NH group. At the anodic potentials where the $Os^{IV}$ imido is generated, the $Os^{II}$ hydrazine complex is further oxidized to the $Os^{V}$ hydrazido(2−). Although the imido reacts under the same conditions with primary amines and with ammonia also, these reactions are not suitable for generating mono- or unsubstituted hydrazido complexes, as these species, once formed, are further oxidized to the $Os^{II}$ dinitrogen complex.

Transition metal hydrazido complexes maintain central importance as models for enzymatic nitrogen fixation. Most of this work has been confined to the electron-rich coordination spheres of molybdenum and tungsten, which readily accommodate the coordination of dinitrogen.[16] Dinitrogen complexes have been protonated to afford hydrazido(2−) complexes, which have in turn been reduced under $N_2$ to yield ammonia and the parent dinitrogen complex. Although the goal of an electrocatalytic cycle has not yet been fully realized, systems have been developed which survive through several cycles of fixation and reduction.[17] Recent efforts have focused on more electron rich environments, in which the expected intermediates, hydrazine and hydrazido(1−) complexes, can be isolated and their decomposition followed in a stepwise manner.[18]

$$W(Cp^*)Me_3(\eta^2\text{-}NH_2NH_2)^+ \xrightarrow{+e^-} W(Cp^*)Me_3(\eta^2\text{-}NH_2NH_2) \rightarrow W(Cp^*)Me_3(NH) + NH_3 \quad (20)$$

The present work shows that the reduction of polypyridyl $Os^{IV}$ dialkylhydrazido(2−) complexes is also a stepwise process. It proceeds through a two-electron intermediate and results in fission of the N−N bond. The first stage of reduction (eq 12) is chemically reversible in neutral and basic solutions, where the putative $Os^{II}$ hydrazine intermediate persists. Recently, $\eta^1$coordination in an $Os^{II}$ hydrazine complex has been established by X-ray crystallography.[19] This complex also undergoes a two-proton, two-electron oxidation,

$$[Os(CO)_2(PPh_3)_2(Br)(NH_2NH_2)]^+ \xrightarrow{Pb(OAc)_4} [Os(CO)_2(PPh_3)_2(Br)(NH{=}NH)]^+ \quad (21)$$

but the product is an $\eta^1$-*trans*-diazene complex.

In the cyclic voltammetry of $[Os(tpy)(bpy)(NH_2NEt_2)]^{2+}$ (Figure 3), the oxidative wave (A) is separated from the reductive wave (I) by nearly 900 mV. The high degree of electrochemical irreversibility of this couple can be attributed to the demands of proton transfer on the electron-transfer kinetics. A similar effect has been observed for the chemically reversible oxidation of $Os^{IV}(tpy)(Cl)_2(NH_3)$ to $[Os^{VI}(tpy)(Cl)_2(N)]^+$, for which oxidative and reductive waves are separated by as much as 1400 mV.[20] The thermodynamic potential of the hydrazido/hydrazine couple,

$$[Os^{IV}(tpy)(bpy)(NNR_2)]^{2+} \underset{-2H^+/2e^+}{\overset{+2H^+/2e^-}{\rightleftharpoons}} [Os^{II}(tpy)(bpy)(NH_2NR_2)]^{2+} \quad (22)$$

estimated from the peak potentials of waves I and A, is −0.20 V at pH 7.0. It exhibits a proton dependence of −62 mV/pH unit over the range $5 < pH < 9$, consistent with a $2H^+/2e^-$ couple. Wave I of Figure 3 may actually be a superposition of two one-electron waves. If so, the reduction is reminiscent of that of polypyridylruthenium oxo complexes such as $[Ru(bpy)_2(py)(O)]^{2+}$, which exhibits two closely spaced waves. We hesitate to make this claim for the present system as the resolution of the two waves is dependent on the composition of the electrolyte and could be due to adsorptive effects. In the second stage of reduction (eq 13), coordinated hydrazine is reduced to ammonia, and the secondary amine is released. This results in the net reversal of the coupling process by which the hydrazido complexes were formed. The appearance of wave E in Figure 3 suggests that capture of the $H_2NR_2^+$ cation is efficient within the confines of the diffusion layer even when the amine is not present in excess.

A complicating factor in the reductive electrochemistry of **2** is the instability of the $Os^{II}$ hydrazine intermediate. It gives rise to an additional pathway for N−N bond cleavage, apart from direct reduction of the hydrazine complex at the electrode. Below pH 6, decomposition is quite rapid, and $[Os(tpy)(bpy)(NH_3)]^{2+}$ is detected in the cyclic voltammetry of **2** after cycling through only the first reductive wave. Our initial observation of kinetics first order in both [Os] and $[H^+]$ led us to suppose that the first step was protonation, followed by rate-determining decomposition of the protonated intermediate, i.e.,

(12) Chatt, J.; Diamantis, A. A.; Heath, G. A.; Hooper, N. E.; Leigh, G. J. *J. Chem. Soc., Dalton Trans.* **1977**, 688.
(13) (a) Kane-Maguire, L. A. P.; Sheridan, P. S.; Basolo, F.; Pearson, R. G. *J. Am. Chem. Soc.* **1970**, *92*, 5865. (b) Lane, B. C.; McDonald, J. W.; Basolo, F.; Pearson, R. G. *J. Am. Chem. Soc.* **1972**, *94*, 3786. (c) Gafney, H. D.; Reed, J. L.; Basolo, F. *J. Am. Chem. Soc.* **1973**, *95*, 7998.
(14) Perez, P. J.; Luan, L; White, P. S.; Brookhart, M.; Templeton, J. L. *J. Am. Chem. Soc.* **1992**, *114*, 7929 and references 1−5 within.
(15) (a) Nugent, W. A.; Haymore, B. L. *Coord. Chem. Rev.* **1980**, *31*, 123. (b) Glueck, D. S.; Hollander, F. J.; Bergman, R. G. *J. Am. Chem. Soc.* **1989**, *111*, 2719, and references 1 and 2 within (17 articles).
(16) (a) McCleverty, J. A. *Transition Met. Chem.* **1987**, *12*, 282. (b) Johnson, B. F. G.; Haymore, B. L.; Dilworth, J. R. In *Comprehensive Coordination Chemistry;* Wilkinson, G., Gillard, R. D., McCleverty, J. A., Eds.; Pergamon Press: Oxford, 1987; Vol. 2, Section 13.3.7. (c) Henderson, R. A.; Leigh, G. J.; Pickett, C. J. *Adv. Inorg. Chem. Radiochem.* **1983**, *27*, 197.
(17) Pickett, C. J.; Ryder, K. S.; Talarmin, J. *J. Chem. Soc., Dalton Trans.* **1986**, 1453.
(18) Schrock, R. R.; Glassman, T. E.; Vale, M. G. *J. Am. Chem. Soc.* **1991**, *113*, 725.
(19) Cheng, T.-Y.; Ponce, A.; Rheingold, A. L; Hillhouse, G. L. *Angew. Chem., Int. Ed. Engl.* **1994**, *33*, 657.
(20) Pipes, D. W.; Bakir, M.; Vitols, S. E.; Hodgson, D. J.; Meyer, T. J. *J. Am. Chem. Soc.* **1990**, *112*, 5507.

$$[Os(tpy)(bpy)(NH_2NR_2)]^{2+} + H^+ \rightleftharpoons [Os(tpy)(bpy)(NH_2NR_2H)]^{3+} \quad (23)$$

$$[Os(tpy)(bpy)(NH_2NR_2H)]^{3+} \rightleftharpoons [Os(tpy)(bpy)(NH)]^{2+} + NH_2R_2^+ \quad (24)$$

$$[Os(tpy)(bpy)(NH)]^{2+} + [Os(tpy)(bpy)(NH_2NR_2)]^{2+} \xrightarrow{fast} [Os(tpy)(bpy)(NH_3)]^{2+} + [Os(tpy)(bpy)(NNR_2)]^{2+} \quad (25)$$

Precedence for eq 24 is found in the decomposition of $MCp^*Me_3(\eta^2\text{-}NH_2NH_2)^+$ (M = Mo, W; $Cp^* = C_5Me_5$), which yields the imido.[21] The reverse reaction in eq 23 is known to be efficient, since it is part of the sequence of reactions by which the hydrazido complexes are formed. However, it was found that throughout the first-order domain, addition of large amounts of $NH_2Et_2^+$ to the reaction mixture did not retard the rate.

Mechanistic investigations of this system are still ongoing. We have not yet arrived at a generalized rate law which describes the decomposition kinetics over an extended pH range. At present, it is valid to conclude only that there are two parallel pathways by which eq 16 is achieved. One involves rate-determining, first-order decomposition of an intermediate which is protonated once with respect to the starting complex. The other pathway is mediated by an unknown catalyst and gives rise to slow, zero-order kinetics when the concentration of protons is low. While added diethylamine does not influence the rate in the first-order domain, at higher pH it suppresses the catalytic branch of the reaction. At pH 9.58, with 0.05 M added diethylamine, $k_{obs}$ is in good agreement with the value extrapolated from lower pH.

Oxidation of **2** occurs *via* two reversible, one-electron steps. The product of the first oxidation (**3**) is a stable compound which can be isolated in solid form, while the product of the second oxidation was observed only on the rapid time scales of cyclic voltammetry. Both in aqueous solution and in acetonitrile, its decomposition affords the $Os^{III}$ solvento complex. When this species, generated by oxidation of **2a**, is allowed to decompose in $CD_3CN$ solution, the organic which forms is the product of carbocation attack on the solvent.[22]

$$C_2H_5^+ + CD_3CN \longrightarrow C_2H_5\text{-}\overset{+}{N}\equiv C\text{-}CD_3 \xrightarrow[-H^+]{+H_2O} C_2H_5\text{-}NH\text{-}\overset{O}{\overset{\|}{C}}\text{-}CD_3 \quad (26)$$

We have considered two possible mechanisms to account for these observations. The first begins with carbocation loss from $Os^{VI}$ (eq 27). Once the first alkyl group is lost, subsequent

$$[Os(tpy)(bpy)(NNR_2)]^{4+} \rightarrow [Os(tpy)(bpy)(NNR)]^{3+} + R^+ \quad (27)$$

$$[Os(tpy)(bpy)(NNR)]^{3+} \rightarrow [Os(tpy)(bpy)(N_2)]^{2+} + R^+ \quad (28)$$

$$[Os(tpy)(bpy)(N_2)]^{2+} \xrightarrow{-e^-} [Os(tpy)(bpy)(N_2)]^{3+} \quad (29)$$

$$[Os(tpy)(bpy)(N_2)]^{3+} \rightarrow [Os(tpy)(bpy)(S)]^{3+} + N_2 \quad (30)$$

$$(S = CH_3CN, H_2O)$$

decomposition proceeds as in eq 9. Potentials sufficient to access the Os(VI/V) wave are also high enough to oxidize $[Os^{II}(tpy)(bpy)(N_2)]^{2+}$ to $Os^{III}$, where dinitrogen is rapidly replaced by solvent (eqs 29 and 30).

A second possibility is that $[Os(tpy)(bpy)(NNR_2)]^{4+}$ may spontaneously solvolyze by loss of the hydrazido ligand,

$$[Os(tpy)(bpy)(NNR_2)]^{4+} + S \rightarrow [Os(tpy)(bpy)(S)]^{3+} + NNR_2^+ \quad (31)$$

with decomposition of $NNR_2^+$ at the anode giving rise to carbocation-addition products.

In the bulk electrolysis experiment, oxidation of **3** consumes *ca.* 2 equiv of electrons, which agrees with the net reaction,

$$[Os(tpy)(bpy)(NNR_2)]^{3+} + CH_3CN \xrightarrow{-e^-} [Os(tpy)(bpy)(NCCH_3)]^{3+} + N_2 + 2R^+ \quad (32)$$

By cyclic voltammetry, the peak height of the second oxidation wave is equal to that of the first, suggesting that on a time-scale of seconds, only one electron is involved in the oxidation of **3**. For the former mechanism, this implies that the alkyldiazonium intermediate of eq 27 is relatively long-lived, which is not consistent with the prompt appearance of the $[Os(tpy)(bpy)(NCCH_3)]^{3+/2+}$ product wave on the return scan. For the latter mechanism, the implication is only that the liberated $NNR_2^+$ fragment (or more likely an intermediate decomposition product) persists for a period of seconds prior to its annihilation at the electrode. We have made no effort to confirm this; however, the decomposition of $[Os(tpy)(bpy)(NNR_2)]^{4+}$ by ligand loss (eq 31) is fully consistent with the electrochemical results and is readily explained on the basis of electronic arguments which are developed later in this section.

Since **2a** and **2c** are the first terminal hydrazides reported for osmium, some discussion of the structures is warranted. Apart from the unusual bent geometry of the $NNR_2$ ligand, both structures are unexceptional. The bipyridine in **2a** and **2c** is bound somewhat asymmetrically, with the Os−N(bpy) bond *trans* to the hydrazido ∼0.1 Å shorter than the bond *cis*. Multiple bonding between osmium and the hydrazido ligand is revealed by short $Os-N_\alpha$ distances in **2a** and **2c**. This distance (1.89 Å for **2a**, 1.84 Å for **2c**) is longer than the 1.78−1.82 Å commonly observed for Mo−N and W−N in linear $NNR_2$ complexes. It is a feature shared by the other three structurally characterized compounds containing the bent hydrazido ligand (M−N = 1.84−1.92 Å).[23] The Os−N−N bond angle of 137° (for **2a** and **2c**) is also within the 131−146° range established by these complexes.

As first noted by Sutton *et al.*, the M−N−N geometry in hydrazido(2−) complexes is such as to allow the maximum number of donated electron pairs consistent with achieving a valence electron count of 18.[11] In the more common linear arrangement, $NNR_2^{2-}$ is a six-electron donor, whereas the bent configuration requires four bonding electrons and one lone pair on $N_\alpha$. The Os−N−N bond angle in **2a** and **2c** indicates that two pairs of electrons ($\sigma + \pi$) are donated to the metal. Moreover, the NNCC units of the hydrazido ligands are planar, suggesting a $\pi$ interaction between nitrogens. The variation in the N−N bond lengths of the osmium complexes is striking. Complex **2c** has the longest N−N bond reported for a hydrazido-

(21) Schrock, R. R.; Glassman, T. E.; Vale, M. G. *J. Am. Chem. Soc.* **1991**, *113*, 725.
(22) The Ritter reaction. See: March, J. *Advanced Organic Chemistry*, 3rd ed.; Wiley: New York, 1985; Chapter 6, p 860.
(23) (a) Jones, T.; Hanlan, A. J. L.; Einstein, F. W. B.; Sutton, D. *J. Chem. Soc., Chem. Commun.* **1980**, 1978. (b) Reference 11. (c) Dilworth, J. R.; Harrison, S. A.; Walton, D. R. M.; Schweda, E. *Inorg. Chem.* **1985**, *24*, 2595.

(2−) complex, while **2a** has the second shortest.[24] This result is surprising, given the similarity of the complexes in other ways. Consistently, however, the N−N stretching frequency in **2c** is 50 $cm^{-1}$ lower than in **2a**. The barrier to rotation about the N−N bond in **2a** is 55.9 kJ $mol^{-1}$ at room temperature. Symetrically substituted *N*,*N*-dialkylhydrazido(2−) ligands are rare, so there is little precedent with which to compare this result. Instances of the *bent* variety were unknown prior to this study. Among *linear* dimethylhydrazido(2−) complexes which contain the molybdenum oxo core, methyl groups can be inequivalent, as in $[Mo(O)(SPh_3)(NNMe_2)]^-$,[25] or equivalent, as in $Mo(O)(dmdtc)_2(NNMe_2)$.[26] In the complex $Mo\{HB(Me_2pz)_3(NO)(I)(NMeNMe_2)\}$, which contains a hydrazido(1−) ligand, the methyl resonances of $N_\beta$ are equivalent at room temperature but separate at low temperature. The barrier to rotation was estimated to be 39 kJ $mol^{-1}$. The hydrazido(1−) complex derived from **2a** exhibits a much larger barrier. Its ethyl groups remain inequivalent up to the decomposition temperature.[27]

We refer to compounds **2** as hydrazido(2−) complexes of $Os^{IV}$ because the dianionic ligand can be formally derived from *N*,*N*-dialkylhydrazine by removal of two protons. This formalism places three unshared electron pairs on the α nitrogen. The bonding picture is completed by allowing one of these to interact with that of the $\beta$ nitrogen, resulting in filled $\pi$ and $\pi^*$ combinations. The $\pi^*$ orbital so formed donates into the vacant $d\pi$ orbital of $Os^{IV}$. The $\pi$ interaction gives rise to the short N−N bond length (1.25 Å for **2a**, 1.40 Å for **2c**) and planarity of the NNCC fragment. However, it is equally valid to envision the bonding as resulting from the interaction of a $\pi$-accepting $NNR_2$ (isodiazene) molecule with $Os^{II}$. Our preference is for the latter description, on the basis of the properties of these molecules.

The electronic absorption spectra of $Os^{II}$ complexes containing bipyridine and terpyridine ligands exhibit strong ($\epsilon \sim 10^5$) metal-to-ligand charge-transfer (MLCT) bands in the visible. This feature is typically not shared by osmium complexes in oxidation state III or higher, whose visible absorptions typically arise from ligand-to-metal charge-transfer (LMCT) or d−d transitions, with MLCT bands appearing at higher energy.[28] In the $Os^{II}$ complexes, stabilization of the metal $d\pi$ orbitals by interaction with $\pi$-acid ligands brings about an increase in the MLCT energy. The effect can be substantial, as demonstrated by the absorption spectrum of $[Os(tpy)(bpy)(NO)](PF_6)_3$ in Figure 4. The powerfully $\pi$ accepting nitrosyl ligand shifts all of the MLCT bands into the near UV.

The complexes $[Os(tpy)(bpy)(NNR_2)]^{2+}$ have intense absorption bands in the visible, and these shift to higher energy when the hydrazido ligand is protonated at $N_\alpha$. If these bands correspond to MLCT transitions, then the observed shift is consistent with the anticipated increase in $\pi$-accepting ability of $NHNR_2^+$ over $NNR_2$. This effect is also apparent in the electrochemistry of the complexes. On protonation, the Os(III/II) wave of **2a** shifts anodically by 1 V and becomes irreversible. This is a direct indication of the instability of the $Os^{III}$ state in the hydrazido(1−) species due to the electron-withdrawing nature of the protonated ligand.

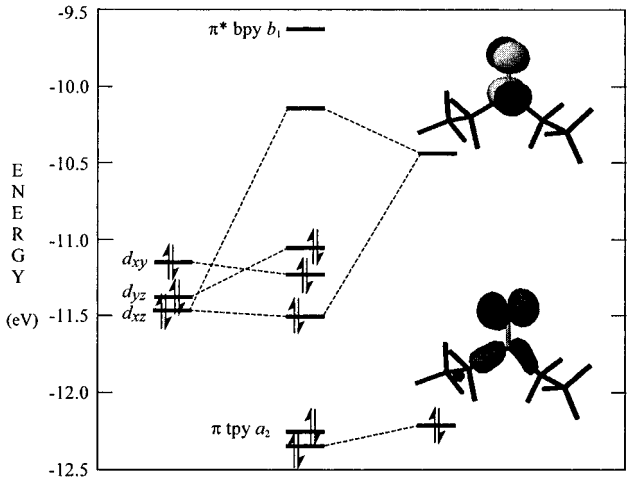


**Figure 5.** Energy level diagram for the cation in **2a**, based on extended Hückel calculations. The *z* axis is the one which passes through Os and $N_\alpha$; the *yz* plane contains Os, $N_\alpha$, and $N_\beta$.

The electronic structure of these systems was further investigated by means of extended Hückel (EH) calculations. The HOMO and LUMO of the diethylisodiazene molecule are represented in Figure 5. The HOMO, in terms of the valence bond model, is a major contributor to the lone electron pairs of $N_\alpha$ and to the C−N $\sigma$ bonds. The LUMO is purely $\pi^*$(NN). When this species becomes a ligand in **2a**, all of its occupied orbitals lie below the $d\pi$ levels of osmium, and $\pi^*$(NN) lies above them. Thus, the formal oxidation state of the metal is +2. The LUMO of the complex cation is largely the same as in the free $NNEt_2$ molecule, but it contains a significant contribution from $d_{xz}$. Accordingly, $d_{xz}$ is not a pure metal-based orbital, but exhibits substantial delocalization onto the isodiazene ligand.

The splitting of the $d\pi$ orbitals is a function of their interaction with the $\pi^*$ orbitals of each of the ligands. The symmetry of $d_{xz}$ allows it to interact with $\pi^*$ levels from three pyridyls and the isodiazene ligand. This orbital lies lowest in energy, immediately below $d_{xy}$ and $d_{yz}$, which is the HOMO. The presence of two filled $d\pi$ levels which do not mix with the orbitals of the isodiazene ligand suggests that both stages of oxidation observed for $[Os(tpy)(bpy)(NNR_2)]^{2+}$ are primarily metal based, *viz.*, Os(III/II) and Os(IV/III). Loss of the back-bonding isodiazene ligand is observed at the $Os^{IV}$ stage, when the $d\pi$ orbitals become too contracted to support $\pi$ bonding. In comparison, oxidation to $Os^{III}$ is sufficient to cause lability of the $\pi$-acid ligands in $[Os(tpy)(bpy)(N_2)]^{3+}$ and $[Os(tpy)(bpy)(NHNR_2)]^{4+}$.

Also borne out in the MO diagram of Figure 5 is the stepwise nature of the reductive chemistry. Reduction by two electrons fills $\pi^*$(NN), reducing the N-N bond order to unity. The parent $p_z$(N) orbitals are no longer constrained to interact, and they degenerate into the two lone electron pairs of hydrazine. Further reduction results in cleavage of the N−N bond.

Because the HOMO is a $d\pi$ orbital that does not mix with $\pi^*$(NN), the EH treatment does not predict a change in N−N bond order on oxidation of **2** to **3**. Experimentally, $\nu_{NN}$ is *ca.* 100 $cm^{-1}$ higher in **3** than in **2**, which may be due to decreased $d\pi + \pi^*$(NN) overlap in the oxidized complex. Since the dependence of orbital extension ($\zeta$) on the atomic charge is not represented in the EH model, we cannot presently elucidate this effect. The same issue arises with the protonation of **2**. The barrier to rotation about N−N is greater in the hydrazido(1−) species than in the hydrazido(2−), suggesting a possible increase

(24) The shortest N−N bond length is reported in the following: Dilworth, J. R.; Zubieta, J. A.; Hyde, P. R. *J. Am. Chem. Soc.* **1982**, *104*, 365.
(25) Burt, R. J.; Dilworth, J. R.; Leigh, G. J.; Zubieta, J. A. *J. Chem. Soc., Dalton Trans.* **1982**, 2295.
(26) Bishop, M. W.; Chatt, J.; Dilworth, J. R.; Hursthouse, M. B.; Montevalli, M. *J. Chem. Soc., Dalton Trans.* **1979**, 1600.
(27) There is another case in which structural isomers were observed for a rhenium hydrazido(1−) but not for the bent hydrazido(2−) from which it was derived (*Inorg. Chem.* **1984**, *23*, 363). In this case, the alkyl substituents of $N_\beta$ are inequivalent, and it is not clear whether protonation increases or decreases the barrier.
(28) (a) Kober, E. M.; Meyer, T. J. *Inorg. Chem.* **1982**, *21*, 3967. (b) Kober, E. M. Ph.D. Dissertation, University of North Carolina at Chapel Hill, 1982.

in the N−N bond order. Although the lone pair which is the site of protonation is not directly tied into the $\pi$ system of the ligand, protonation affects the amount of positive charge residing on the metal. Overlap between d$\pi$ and $\pi$*(NN) may play a role here as well.

While the origin of the 700−800 $cm^{-1}$ bands in the Raman spectra of these species has not been uniquely determined, it is clear from their resonance enhancements that these modes are strongly coupled to the transition between ground and excited states. If the bands correspond to the Os−$N_\alpha$ stretch coupled to other modes, and if the electronic transition is MLCT in character, a large resonance enhancement is indeed expected on the basis of the influence of the oxidation state of the metal on equilibrium bond lengths. An Os−N stretching frequency in the 700−800 $cm^{-1}$ range is suggestive of substantial metal−ligand multiple bonding which, according to the isodiazene description, must be a result of the back-bonding interaction.

**Acknowledgment.** The authors are deeply appreciative of Dr. John C. Brewer and Dr. Durwin Striplin for their helpful discussions and Dr. William M. Davis (MIT) for solution and refinement of the structure of **2a**. We gratefully acknowledge the National Institutes of Health for supporting this research through Grant No. 5-RO1-GM-32296-05.

**Supporting Information Available:** Tables of collection and refinement parameters, positional and thermal parameters, bond distances, and bond angles for **2a** and **2c**, background-subtracted cyclic voltammograms of **2a** recorded at pH 5.0, cyclic voltammograms of **2a** recorded in $CH_3CN$ with 0.1 M TBAH at a scan rate of 100 mV/s and resonance-Raman spectra of **2a** in 6.0 M HCl and 6.0 M DCl solutions (35 pages). Ordering information is given on any current masthead page.

IC961025V